Strong Effect of Resonant Impurities on Landau-Level Quantization

G. Allison,[1] N. Mori,[1,2] A. Patanè,[1,*] J. Endicott,[1] L. Eaves,[1] D. K. Maude,[3] and M. Hopkinson[4]

[1]*School of Physics and Astronomy, University of Nottingham, Nottingham NG7 2RD, United Kingdom*
[2]*Department of Electronic Engineering, Osaka University, 2-1 Yamada-Oka, Suita City, Osaka 565-0871, Japan*
[3]*Grenoble High Magnetic Field Laboratory, C.N.R.S, Grenoble, F-38042, France*
[4]*Department of Electronic and Electrical Engineering, University of Sheffield, Sheffield, S3 3JD, United Kingdom*

(Received 6 February 2006; published 12 June 2006)

We investigate experimentally the effect of a random distribution of nitrogen (N) impurities on the Landau-level spectrum of a GaAs quantum well. Our magnetotunneling study reveals complex and nonequally spaced Landau levels and a quenching of the Landau states at a well-defined bias and electron energy which is resonant with that of the N atoms. Analysis of the magnetic field dependence of the tunnel current into the Landau levels of the well also provides quantitative information about the nonresonant component of the N-related scattering potential.

DOI: 10.1103/PhysRevLett.96.236802 PACS numbers: 73.40.Gk, 73.21.−b, 73.61.Ey, 73.43.Fj

The Landau-level quantization of the electronic states of semiconductors by a strong magnetic field has provided the condensed matter physicist with a powerful means of probing fundamental quantum phenomena [1], such as the integer quantum Hall effect [2]. The effect of disorder on the Landau levels (LLs) has played a key role in understanding this and other phenomena. Work has focused on different types of disorder potential [3–6] and particularly that caused by a random distribution of nonresonant scattering centers. In this case, the disorder lifts the degeneracy of each LL to form a broad energy band containing localized and extended electronic states. However, recent developments have made it possible to realize epitaxial structures in which the energy of the localized states associated with the scattering centers is resonant with extended continuum states [7,8]. These systems include *mismatched* III-V semiconductor alloys doped with highly electronegative N impurities which have an energy level, E_N, in resonance with the conduction band states of the host lattice [9]. The effect of this type of scatterer on Landau-level quantization is still largely unexplored.

Here we investigate the quantized LL states in a GaAs quantum well (QW) containing a small concentration (1 part per 1000) of randomly distributed N impurities. Our tunneling spectroscopy measurements reveal the presence of nonequally spaced LLs and a quenching of the Landau states at energies close to E_N. In addition, our analysis of the measured magnetic field dependence of the tunnel current into the lower energy LL states of the QW allows us to quantify the strength and spatial extent of the nonresonant component of the N-related scattering potential. Our results are of general interest as the magnetotunneling technique could be used to probe other types of disordered potential. They are also relevant to novel devices based on III-N-V alloys that have potential for long-wavelength telecommunications [10,11] and high-frequency electronics [12].

For our study, we use $GaAs/Al_{0.4}Ga_{0.6}As/Ga(AsN)$ resonant tunneling diodes grown by molecular beam epitaxy on (001)-oriented Si-doped GaAs substrates. The sample that we examine in detail here contains an 8 nm wide Ga(AsN) QW layer with $N \sim 0.1\%$ embedded between two 6 nm wide $Al_{0.4}Ga_{0.6}As$ tunnel barriers; undoped GaAs spacer layers of width 50 nm separate the $Al_{0.4}Ga_{0.6}As$ barriers from the Si-doped GaAs layers [13]. The samples were processed into mesas with a diameter of 100 μm and with a ring-shaped metallic top contact layer to provide optical access for current-voltage, *I-V*, measurements under illumination. Throughout this Letter, positive bias corresponds to the top Si-doped capping layer biased positively.

By tuning the voltage between the top and bottom Si-doped GaAs layers, the energy of a quantized subband of the QW can be aligned with that of the occupied states in the emitter layer [Fig. 1(a)]. This gives rise to resonant tunneling of electrons and to a series of peaks in *I-V*. In a

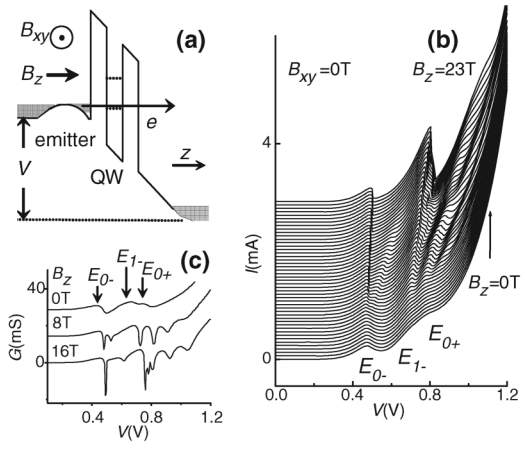

FIG. 1. (a) Schematic band diagram of our resonant tunneling diode. (b) *I-V* at $T = 4.2$ K and various B_z; B_z is increased from 0 to 23 T in steps of 0.5 T. (c) Differential conductance, $G(V)$, plots for $B_z = 0, 8, 16$ T. For clarity, the curves are displaced along the vertical axis. The sample was illuminated with laser light of wavelength $\lambda = 633$ nm at a power density <0.01 W/cm^2.

previous paper [13], we showed that by applying a magnetic field, B_{xy}, parallel to the QW plane, xy, an electron can be tuned to tunnel into a state of in-plane wave vector, k, of the QW subband; by tuning the electron energy, ε, with the applied bias, this experiment mapped out the energy dispersion curves, $\varepsilon(k)$, of the lowest energy subbands, E_{0-}, E_{1-} and E_{0+} of the QW [Fig. 2(a)]. These subbands arise from the hybridization of the unperturbed QW subbands, E_0 and E_1, of the GaAs host matrix with the localized N-resonant state. Around $k = 0$, subbands E_{0-}, E_{1-} exhibit a dominant bandlike character, while E_{0+} has a significant impurity-N-like nature [13]. For this configuration of magnetic field, LL quantization of the QW subbands does not occur since the quantum confinement provided by the two tunnel barriers is dominant.

We now focus on the configuration in which the magnetic field is applied along z or tilted by an angle θ relative to z. For $\theta = 0°$, the magnetic field, B_z, quantizes the electron motion in the QW plane into LLs. In the absence of scattering, electrons should tunnel from the emitter into the QW with conservation of the LL index, n [14]; this corresponds to conservation of the in-plane wave vector for the case $B_z = 0$. By tilting the magnetic field axis relative to z, it is possible to switch on otherwise "forbidden" quantum transitions, which involve a change in n [15,16].

Figure 1(b) shows the I-V characteristics at $T = 4.2$ K at different B_z. At $B_z = 0$ T, the I-V curve shows resonant features E_{0-}, E_{1-} and E_{0+}. A strong enhancement and narrowing of the resonances is observed as B_z is increased above about 5 T. For $B_z > 5$ T, the I-V are also modulated by additional features, which are more clearly revealed in the plots of the differential conductance, $G(V) = dI/dV$ [Fig. 1(c)]. To track the voltage position and amplitude of the resonances with increasing B_z, in Fig. 2(b) we show a gray-scale plot of the intensity of G versus B_z and V. In this plot, the white stripelike regions correspond to the minima of G just beyond the resonant peak in I-V. The stripes provide a clear, sharp marker of the resonances since the current falls abruptly when the bias is increased beyond the peak of the current [13].

The enhancement and sharpening of the resonances with increasing B_z is a "density-of-states" effect caused by the discrete nature and high degeneracy of the LLs. Our data also reveal a LL splitting pattern, which is relatively simple in the low bias region around the E_{0-} resonance. Resonance E_{0-} splits into two distinct features, which shift linearly with increasing B_z. We attribute these to tunneling transitions involving elastic or quasielastic scattering from the lowest ($n = 0$) LL in the emitter layer into the first two LLs of the E_{0-} subband. In Fig. 2(b) we label these two resonances with the LL index change, $\Delta n = 0$ and 1. Note that the $\Delta n = 1$ feature, which would be forbidden in the absence of scattering, is weaker than that with $\Delta n = 0$, but is nevertheless clearly discernible over a wide range of B_z. The dependence on B_z of the higher bias ($V > 0.6$ V) resonances is instead more complicated and strongly nonlinear. However, at B_z (>10 T), a fanlike series of features emerges in the gray-scale plots, with the voltage positions shifting steadily upward with increasing B_z.

Both the intensities and voltage positions of all the resonances in I-V are modified by tilting the magnetic field, B_θ, at an angle θ to the z direction [Figs. 2(c) and 2(d)]. Tilting the field decreases the intensity of the features with weak magnetic field dependence (corresponding to no change in n) relative to those with a strong magnetic field shift. Note that the $\Delta n = 0$ resonance of E_{0-} decreases in amplitude, while the $\Delta n = 1$ resonance is enhanced, together with a new feature due to electron tunneling into a LL with $n = 2$ [Fig. 2(d)].

These data reveal a complicated LL fan diagram and an unusual quenching of the LL features at a well-defined bias, which corresponds to an electron tunneling close to the energy, E_N, of the N level [see horizontal arrow in Figs. 2(a) and 2(d)]. As discussed below, this information combined with the measured intensity of the transitions at different B_θ provides us with a means of probing the N-related scattering potential.

We model our magnetotunneling experiment using a sequential tunneling analysis illustrated schematically in Fig. 3(a). We divide the system into three subsystems: a two-dimensional (2D) emitter, a QW, and a 3D collector. The tunneling from the QW to the 3D collector is assumed to be a nonresonant process so that the observed resonant features in I-V arise entirely from tunneling transitions

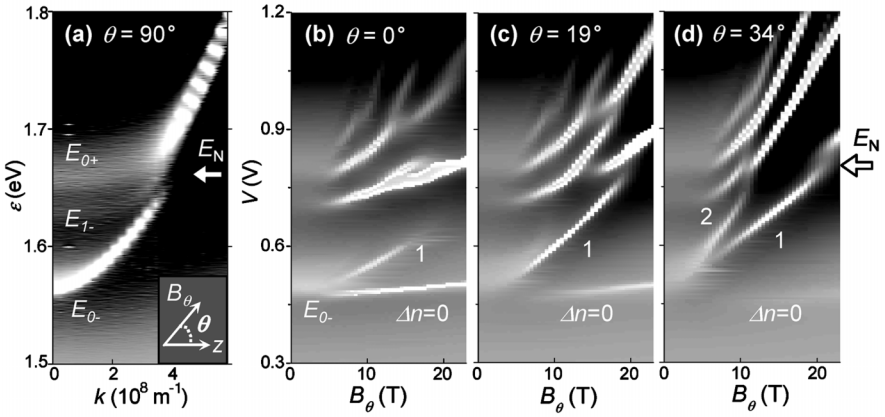

FIG. 2. (a) Energy dispersion relations, $\varepsilon(k)$, for a Ga(AsN) QW as derived from magnetotunneling experiments with magnetic field, B_θ, parallel to the QW plane ($\theta = 90°$). The inset shows the definition of θ. (b)–(d) Gray-scale plots of the differential conductance, G, vs V and B_θ. (b) $\theta = 0°$; (c) $\theta = 19°$; (d) $\theta = 34°$.

from the 2D emitter into the QW. Each subsystem is described by a Hamiltonian that includes the effect of both components of B_θ, namely, the LL quantization arising from B_z and the symmetry breaking effect of B_{xy}. For the QW states, we use a band anticrossing model that considers the hybridization of the GaAs Γ-conduction QW subband states with the localized N-resonant level [8,9].

We consider first the purely "ballistic" component of the electron tunnel current in which electrons tunnel from the emitter into the QW with no scattering. The tunnel current, I_0, is proportional to the product of the squares of the moduli of the Bardeen transfer matrix element [17] and the in-plane tunneling matrix element, M_0, between the emitter and QW states, i.e., $M_0 = \langle \varphi_w^{xy} | \varphi_e^{xy} \rangle$, where $|\varphi_e^{xy}\rangle$ and $|\varphi_w^{xy}\rangle$ are the wave functions for electrons in the emitter and QW layers, respectively. Scattering of tunneling electrons by the disorder introduces an additional contribution, I_1, given by the modulus squared of the matrix element, $M_1 = \langle \varphi_w^{xy} | U | \varphi_e^{xy} \rangle$, where U is the scattering potential seen by the electrons as they tunnel in the QW. In our calculation $U(\mathbf{r}) = U_0 \sum_{j=1}^{P} e^{-|\mathbf{r}-\mathbf{r}_j|^2/d^2}$, where d and U_0 represent, respectively, the characteristic length scale and strength of the scattering potential. The sum is taken over a randomly distributed set of P points located at $\mathbf{r}_j$ in the xy plane.

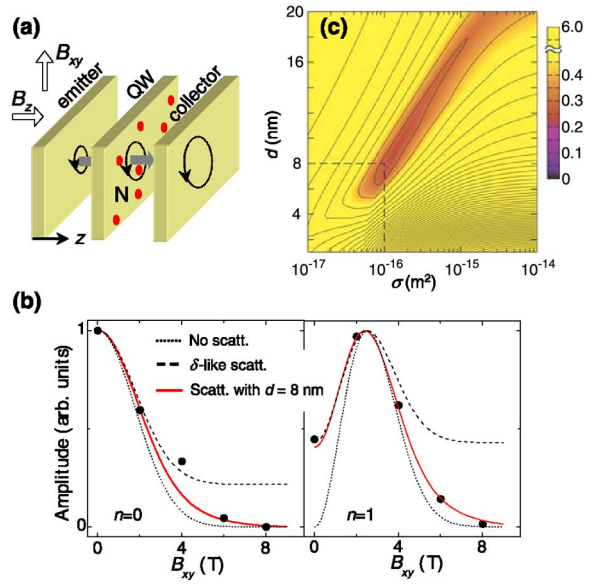

FIG. 3 (color online). (a) Schematic diagram describing the sequential tunneling model. (b) Dependence on B_{xy}, at constant $B_z = 12$ T, of the amplitude of the resonant features $\Delta n = 0$ and 1 in the dG/dV plots. The dots are the experimental data. The lines are the calculated curves for the case of ballistic tunneling (dotted line), short-range delta-function-like scatterers (dashed line), and finite range scatterers with $d = 8$ nm and $\sigma = 10^{-16}$ m^2 (solid line). (c) Color plot and associated contours versus d and σ of the quantity $R = \sum_i R_i$, where R_i is the difference between a data point (i) and the calculated curve shown in part (b). The analysis of the experimental data is based on two fitting parameters σ and d. By using the independently determined value of $\sigma = 10^{-16}$ m^2 (see vertical dashed line), the best fit to the measured data is obtained with $d = (8 \pm 2)$ nm (see horizontal dashed line).

Our model indicates that the tunnel current depends sensitively on the parameters P, d and U_0. At $B_{xy} = 0$, the intensity ratio between the $\Delta n = 0$ and 1 transitions can be expressed as $I_{\Delta n=1}/I_{\Delta n=0} = \sigma/(\pi l_z^2 + \sigma)$, where $l_z = (\hbar/eB_z)^{1/2}$ is the magnetic length and $\sigma = 0.5\rho m^2 \hbar^{-4} \xi^2 U_0^2 \pi^2 d^4 t^2$. Here m is the electron effective mass in AlAs, t is the thickness of the tunnel barrier, ξ is the penetration length into the barrier of the wave-function of electrons in the emitter ($\xi = 1$ nm) and $\rho = P/S$, where S is the mesa area. By fitting to our measured value of $I_{\Delta n=1}/I_{\Delta n=0}$ at $B_z = 12$ T, we obtain $\sigma = 10^{-16}$ m^2. We can now incorporate this value of σ into our analysis of the tilted field data.

Figure 3(b) compares our measured plots of the intensity of the $\Delta n = 0$ and 1 LL features in the dG/dV plots as a function of B_{xy} and constant $B_z = 12$ T with the calculated dependences derived from our model assuming different forms of the scattering potential. In this configuration of magnetic field, the effect of the B_{xy} component is to provide the tunneling electron with an additional in-plane component of wave vector, k_β, which breaks the orthogonality of the initial and final LL states with different values of n [15,16]. In the absence of scattering, the calculated curves [see dotted lines in each box of Fig. 3(b)] have the form expected for the wave-function probability density in k space of the electron in the $n = 0$ and $n = 1$ LLs since the tunneling matrix element, M_0, can be expressed in terms of the Fourier transforms $\varphi_{e(w)}^{xy}(k)$, of the real space LL wave functions of the emitter and QW, i.e., $M_0 = \int_k \varphi_e^{xy}(k - k_\beta)\varphi_w^{xy}(k)dk$. Here, $k_\beta = eB_{xy}s/\hbar$ is the k vector gained by an electron tunneling across the barrier into the QW and s is the effective tunneling distance from the emitter to the center of the well. The calculated curves describe qualitatively our measured data. However, note that the measured intensity of the $\Delta n = 1$ LL feature at $B_{xy} = 0$ is nonzero. This identifies the presence of a scattering-related contribution to the measured tunneling current.

We can determine the nature of the scattering potential by noting that the precise form of the B_{xy} dependence of the $\Delta n = 0$ and 1 LL transitions is very sensitive to d. As can be seen in Fig. 3(b) (see dashed lines), for a random distribution of short-range delta-function-like scatterers, the calculated amplitude of the tunnel transitions remains large even at high B_{xy} (>5 T), which is not consistent with our data. To determine d, we use the procedure shown in Fig. 3(c). Here the color plot and associated contours in the d-σ parameter space quantify the fit between our model and the data points in Fig. 3(b). Using the value of $\sigma = 10^{-16}$ m^2 deduced from the independent measurement of $I_{\Delta n=1}/I_{\Delta n=0}$ at $B_z = 12$ T, we obtain $d = (8 \pm 2)$ nm [see lines in Fig. 3(b)]. This value of d is considerably larger than the calculated radius of the highly localized and resonant eigenfunction associated with the N atoms (~1 nm)

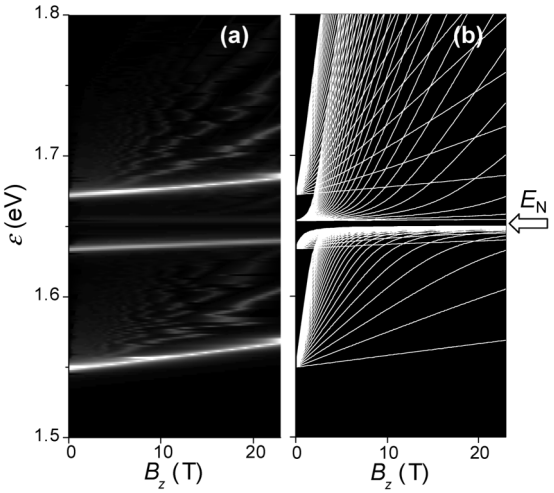

FIG. 4. (a) Calculated gray-scale plots of current I vs energy ε and B_z ($\theta = 0°$). (b) Calculated dependence of the LL energy ε on B_z. The energy is plotted relative to the valence band of GaAs at $T = 4.2$ K.

[18]. However, it is consistent with the length scale expected for local fluctuations in the N content at low N concentrations (~0.1%) [19]. This result can be understood by noting that the energy of the electrons which resonantly tunnel into the first two LLs of the E_{0-} QW subband are well below the resonant energy associated with the individual N atoms in GaAs. Hence the Fourier component $U(k)$ of the scattering potential, which determines the scattering-induced current should correspond to relatively small wave vectors, considerably smaller than those arising from the highly localized part of the N-impurity potential. The amplitude of the scattering potential, U_0, is estimated by using the expression for σ with values of d and σ derived from our analysis and assuming that $P\pi d^2 \leq S$. This gives $U_0 \geq 120$ meV, which indicates a strong perturbation in the potential of the well due to the randomly distributed and highly electronegative N atoms [19].

We now consider the complex series of LL features corresponding to energies closer to that of the N level. Our calculated gray-scale plot in Fig. 4(a) indicates that the N atoms act to resonantly quench the LLs at a well-defined energy, E_N, where admixing and hybridization of extended and localized states occurs, thus resulting in a strong suppression of the Γ-like character of the states [9]. This is in qualitative agreement with the measured gray-scale plot of Fig. 2(b). Also, note that the calculated energy of the LLs have a strongly nonlinear dependence on B_z [see Fig. 4(b)]. This is caused by the unusual form of the $\varepsilon(k)$ dispersions and corresponding strong dependence of the electron cyclotron effective mass upon energy and hence upon B_z. Although our calculated LL spectrum does not replicate the measured LL splitting, there are qualitative similarities to the measured plot: the LLs maintain a linear dependence on B_z over an extended range of energies and deviate from it only at energies close to E_N; also the apparent forking of the LLs for $V > 0.7$ V and $B_z \sim 10$ T in Fig. 2(b) resembles the form of the calculated LL splitting above E_N.

In conclusion, our magnetotunneling experiment in a GaAs quantum well incorporating N scatterers shows that the LL levels are admixed and are quenched at energies close to the resonance state of the individual N impurities. For the energy range below the N level, we demonstrate that our analysis of the magnetic field dependence of the tunnel current provides quantitative information about the length scale and amplitude of the nonresonant component of the N-related scattering potential.

We thank the Engineering and Physical Sciences Research Council (UK) for support.

*Corresponding author.
Electronic address: Amalia.Patane@nottingham.ac.uk

[1] T. Ando, A. B. Fowler, and F. Stern, Rev. Mod. Phys. **54**, 437 (1982).
[2] K. von Klitzing, G. Dorda, and M. Pepper, Phys. Rev. Lett. **45**, 494 (1980).
[3] R. J. Haug, R. R. Gerhardts, K. V. Klitzing, and K. Ploog, Phys. Rev. Lett. **59**, 1349 (1987).
[4] K. A. Benedict and J. T. Chalker, J. Phys. C **18**, 3981 (1985); **19**, 3587 (1986).
[5] M. E. Raikh and T. V. Shahbazyan, Phys. Rev. B **47**, 1522 (1993).
[6] T. V. Shahbazyan and S. E. Ulloa, Phys. Rev. B **57**, 6642 (1998).
[7] K. Karrai *et al.*, Nature (London) **427**, 135 (2004).
[8] W. Shan *et al.*, Phys. Rev. Lett. **82**, 1221 (1999).
[9] A. Lindsay and E. P. O'Reilly, Phys. Rev. Lett. **93**, 196402 (2004).
[10] L. Lombez *et al.*, Appl. Phys. Lett. **87**, 252115 (2005).
[11] A. R. Adams, Electron. Lett. **40**, 1086 (2004).
[12] A. Patanè *et al.*, Phys. Rev. B **72**, 033312 (2005).
[13] A. Patanè *et al.*, Phys. Rev. B **71**, 195307 (2005).
[14] M. L. Leadbeater *et al.*, Phys. Rev. B **39**, 3438 (1989).
[15] Y. Galvao Gobato *et al.*, Phys. Rev. B **44**, 13 795 (1991).
[16] M. L. Leadbeater, F. W. Sheard, and L. Eaves, Semicond. Sci. Technol. **6**, 1021 (1991).
[17] A. Patanè *et al.*, Phys. Rev. B **65**, 165308 (2002).
[18] P. R. C. Kent and A. Zunger, Phys. Rev. B **64**, 115208 (2001).
[19] The length, l_s, expected for fluctuations in the small number of N atoms, which scatter the electrons tunneling into the QW, can be estimated using a simple statistical argument. The expected fluctuation, Δx, in the concentration of N atoms around a means value x is $\Delta x = \sqrt{a^3 x/4V}$. Here a is the GaAs lattice constant ($a = 0.56$ nm) and V is the volume probed by the electron. This is given by $V = \xi l_s$, where ξ is the penetration length into the barrier of the wave function of electrons in the emitter ($\xi = 1$ nm). Assuming $\Delta x \sim x = 0.1\%$, we derive $l_s = \sqrt{a^3/4\xi x} = 7$ nm. Using a two-level band anticrossing model, we estimate that the characteristic energy fluctuation, ΔE, of the conduction band minimum of Ga(AsN) induced by compositional fluctuations is $\Delta E = (\partial E/\partial x)x \sim \pm 25$ meV for $x = 0.1\%$.